Journal of Engineering Physics and Thermophysics, Vol. 78, No. 4, 2005

FUNCTIONAL IDENTIFICATION OF THE NONLINEAR THERMAL-CONDUCTIVITY COEFFICIENT BY GRADIENT METHODS. II. NUMERICAL MODELING

V. T. Borukhov,[a] V. I. Timoshpol'skii,[b] G. M. Zayats,[a] and V. A. Tsurko[a]

UDC 519.6

Algorithms for the gradient method of solution of the inverse problem on determination of the nonlinear thermal-conductivity coefficients are given. Results of numerical experiments are discussed.

Introduction. In [1], we consider the problem of functional identification of the nonlinear thermal-conductivity coefficient $\lambda(T)$. Behind the approach proposed is the gradient method of numerical solution of inverse heat-conduction problems [2–4]. We note that, in the traditional approach to finding $\lambda(T)$, one uses a finite-dimensional approximation of a coefficient by the system of basis functions [4], whereas in [1], we propose a method of solution of inverse heat-conduction problems without preliminary approximation of the functions sought; this method uses new representations of the operator conjugate to the internal-superposition operator, which makes it possible to obtain formulas convenient for numerical calculations of the values of the conjugate operator.

In the present work, we propose algorithms of functional identification of the coefficient $\lambda(T)$, describe computational experiments, and discuss calculation results.

Computational Formulas. We give the formulas from [1], which are necessary for numerical realization of the algorithms of solution of inverse heat-conduction problems. The system of equations for finding $\lambda(T)$ has the form

$$c(T)\frac{\partial T}{\partial t}=\frac{\partial}{\partial x}\left(\lambda(T)\frac{\partial T}{\partial x}\right),$$

$$T(x,0)=T_0(x),\quad T(0,t)=g_1(t),\quad T(b,t)=g_2(t), \tag{1}$$

$$y(t)=T(x_*,t).$$

Here $(x, t) \in \Omega = [0, b] \times [0, t_f]$ and $T_0(x)$, $g_1(t)$, $g_2(t)$, and $y(t)$ are the prescribed formulas. The point x_* lies within the segment $[0, b]$. The approximations of the function $\lambda(T)$ are prescribed by the recurrence system

$$\lambda_{n+1}=\lambda_n-\beta_n l_n,$$

$$l_n=J'_{\lambda_n}-\gamma_{n-1}l_{n-1},\quad l_0=J'_{\lambda_0}, \tag{2}$$

where λ_0 is the initial approximation, the parameter γ_{n-1} is determined by the equality $\gamma_{n-1}=\dfrac{\|J'_{\lambda_n}\|^2_\Lambda}{\|J'_{\lambda_{n-1}}\|^2_\Lambda}$, $\beta_n=\dfrac{-\int_0^{t_f} p_n(s)\nu(x_*,s)ds}{\int_0^{t_f}\nu^2(x_*,s)ds}$, $\|\cdot\|_\Lambda$ is the norm in the Hilbert space $L_2[T^{(1)}, T^{(2)}]$ of functions summable with the square on the

[a]Institute of Mathematics, National Academy of Sciences of Belarus, 11 Surganov Str., Minsk, 220072, Belarus; [b]A. V. Luikov Heat and Mass Transfer Institute, National Academy of Sciences of Belarus, Minsk, Belarus. Translated from Inzhenerno-Fizicheskii Zhurnal, Vol. 78, No. 4, pp. 75–81, July–August, 2005. Original article submitted February 2, 2005.

1062-0125/05/7804-0703

segment $[T^{(1)}, T^{(2)}]$ or the norm in Sobolev's Hilbert space $W_2^1[T^{(1)}, T^{(2)}]$ of functions absolutely continuous on the segment $[T^{(1)}, T^{(2)}]$, and ν is the solution of the initial boundary-value problem

$$\frac{\partial}{\partial t}(c(T_n)\nu) = \frac{\partial^2}{\partial x^2}(\lambda_n(T_n)\nu) + \frac{\partial}{\partial x}\left(l_n \frac{\partial T_n}{\partial x}\right),$$
$$\nu(0, t) = \nu(b, t) = 0, \quad \nu(x, 0) = 0; \tag{3}$$

T_n is the solution of problem (1) for $\lambda(T) = \lambda_n(T_n)$; $p_n(t) = T_n(x_*, t) - y(t)$.

The problem conjugate to (3) has the form

$$c(T_n)\frac{\partial w}{\partial t} + \lambda_n(T_n)\frac{\partial^2 w}{\partial x^2} - \delta(x - x_*)\, p_n(t) = 0,$$
$$w(x, t_f) = 0, \quad w(0, t) = w(b, t) = 0. \tag{4}$$

According to [1], the gradient J'_{λ_n} may be determined from one of the following relations:

$$J'^{1}_{\lambda_n} = -\frac{d}{dz}\int_0^b \int_0^{t_f} \chi(z, T_n(x, t))\frac{\partial T_n(x, t)}{\partial x}\frac{\partial w(x, t)}{\partial x}\, dt dx \equiv -\frac{d}{dz}\int_\Omega R(z, x, t)\frac{\partial T_n(x, t)}{\partial x}\frac{\partial w(x, t)}{\partial x}\, dx dt, \tag{5}$$

$$J'^{2}_{\lambda_n} = -\int_\Omega \frac{\partial T_n(x, t)}{\partial x}\frac{\partial w(x, t)}{\partial x}\, dx dt - \int_{T^{(1)}}^{z}\int_\Omega r(\tau, x, t)\frac{\partial T_n(x, t)}{\partial x}\frac{\partial w(x, t)}{\partial x}\, dx dt d\tau, \tag{6}$$

$$J'^{3}_{\lambda_n} = -\int_\Omega \frac{\partial T_n(x, t)}{\partial x}\frac{\partial w(x, t)}{\partial x}\, dx dt - \int_{z}^{T^{(2)}}\int_\Omega R(\tau, x, t)\frac{\partial T_n(x, t)}{\partial x}\frac{\partial w(x, t)}{\partial x}\, dx dt d\tau. \tag{7}$$

Here $\chi(z, s) = \begin{cases} 1 & \text{for } T^{(1)} \le s \le z, \\ 0 & \text{for } z \le s \le T^{(2)} \end{cases}$ is the characteristic function of the set $\{s \mid T^{(1)} \le s \le z\}$, $T^{(1)} = \min\limits_{(x,t)\in\partial\Omega} T(x, t)$ and $T^{(2)} = \max\limits_{(x,t)\in\partial\Omega} T(x, t)$ and $R(z, x, t)$ and $r(\tau, x, t)$ are the characteristic functions of the sets $\omega(z) = \{(x, t) \in \Omega \mid T_n(x, t) \le z \le T^{(2)}\}$ and $\bar{\omega}(\tau) = \Omega \setminus \omega(\tau) = \{(x, t) \in \Omega \mid T^{(1)} \le \tau \le T_n(x, t)\}$ respectively.

The norm of the gradient J'_{λ_n} is found as

$$\|J'^{1}_{\lambda_n}\|^2_{L_2} = \int_{T^{(2)}}^{T^{(1)}} \left(J'^{1}_{\lambda_n}\right)^2 dz, \quad \|J'^{i}_{\lambda_n}\|^2_{W_2^1} = \left(\int_\Omega \frac{\partial T_n(x, t)}{\partial x}\frac{\partial w_n(x, t)}{\partial x}\, dx dt\right)^2 + \int_{T^{(1)}}^{T^{(2)}} l_{ni}^2\, dz, \quad i = 2, 3, \tag{8}$$

where

$$l_{n2} = \int_\Omega r(\tau, x, t)\frac{\partial T_n(x, t)}{\partial x}\frac{\partial w(x, t)}{\partial x}\, dx dt; \quad l_{n3} = \int_\Omega R(z, x, t)\frac{\partial T_n(x, t)}{\partial x}\frac{\partial w(x, t)}{\partial x}\, dx dt. \tag{9}$$

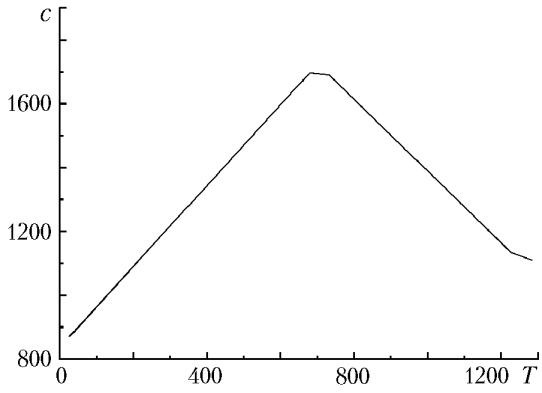

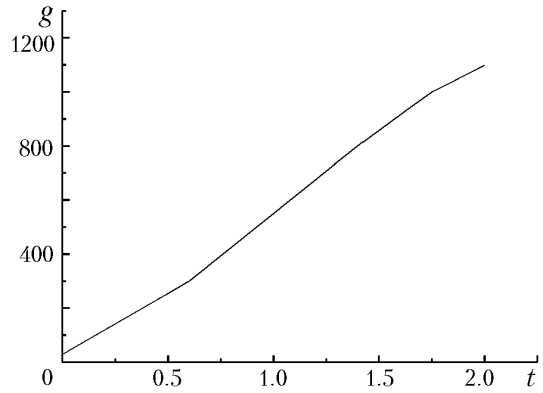

Fig. 1. Heat-capacity coefficient vs. temperature. c, W·h/(m^3·^{o}C); T, ^{o}C.

Fig. 2. Boundary values of temperature vs. time. $g(t)$, ^{o}C; t, h.

In describing computational experiments, the variants of the algorithm (2) (I, II, and III) will correspond to the numbers i = 1, 2, and 3 in the notation $J'_{\lambda_n^i}$.

Results of Computational Experiments. Difference methods presented in [5] have been used for numerical solution of the initial boundary-value problems (1), (3), and (4). The integrals in (5)–(9) were computed by the standard trapezium method. Also, we used the procedure of restoration of the iteration process (2) in the case of increase in the residual on the nth + 1 iteration (the procedure involved the selection of $\lambda_n(T)$ as the initial approximation λ_0 and subsequent solution of problems (1), (3), and (4) with a new initial approximation.

The numerical experiment was carried out for the model functions $\lambda(T) = \lambda_m(T)$ of the form

$$\lambda_m(T) = -0.02T + 50.0\,, \tag{10}$$

$$\lambda_m(T) = \begin{cases} 0.023T + 34.67 & \text{at } T \in [30^o\text{C}, 700^o\text{C}]\,; \\ -0.045T + 81.82 & \text{at } T \in [700^o\text{C}, 1200^o\text{C}] \end{cases} \tag{11}$$

with different initial approximations λ_0 and at different points x_* of measurement of the temperature.

For the calculations, we selected the parameters b = 0.27 m and t_f = 2.0 h. The results have been obtained for the number of nodes N_x = 55 in the spatial variable and the number of nodes N_t = 200 in the temporal variable; from the conditions of approximation of the delta function in (4), the point x_* coincides with the grid node. The behavior of the functions $c(T)$ [6] and $g_1(t) = g_2(t) = g(t)$ [7] is shown in Figs. 1 and 2. The computation results are presented in Figs. 3–7. In computing $\lambda(T)$, we used both the accurate input data and noise-affected data.

Figure 3 gives numerical calculations of the thermal-conductivity coefficient at different points x_*. Figure 3a presents results of restoration of $\lambda(T)$ according to algorithm I. We note that in this case selection of the point x_* makes it impossible to attain satisfactory relations $\lambda_n(T^{(1)}) \approx \lambda_m(T^{(1)})$ and $\lambda_n(T^{(2)}) \approx \lambda_m(T^{(2)})$ for the boundary values of temperature and for fairly large n. The results of calculations according to algorithm II (Fig. 3b) show that the $\lambda_n(T^{(2)})$ values are satisfactory at $T = T^{(2)}$, whereas we were unable to substantially improve the $\lambda_n(T^{(1)})$ values. Figure 3c illustrates the operation of algorithm III.

Figure 4 presents the overlap of the results of restoration of the thermal-conductivity coefficient according to the three algorithms for the model problem selected. Figure 5 gives results of restoration of $\lambda(T)$ with the derivative (11) discontinuous in T, which have been found for different values of the residual

$$\varepsilon_n = \int_0^{t_f} p_n(s)^2\, ds\,, \tag{12}$$

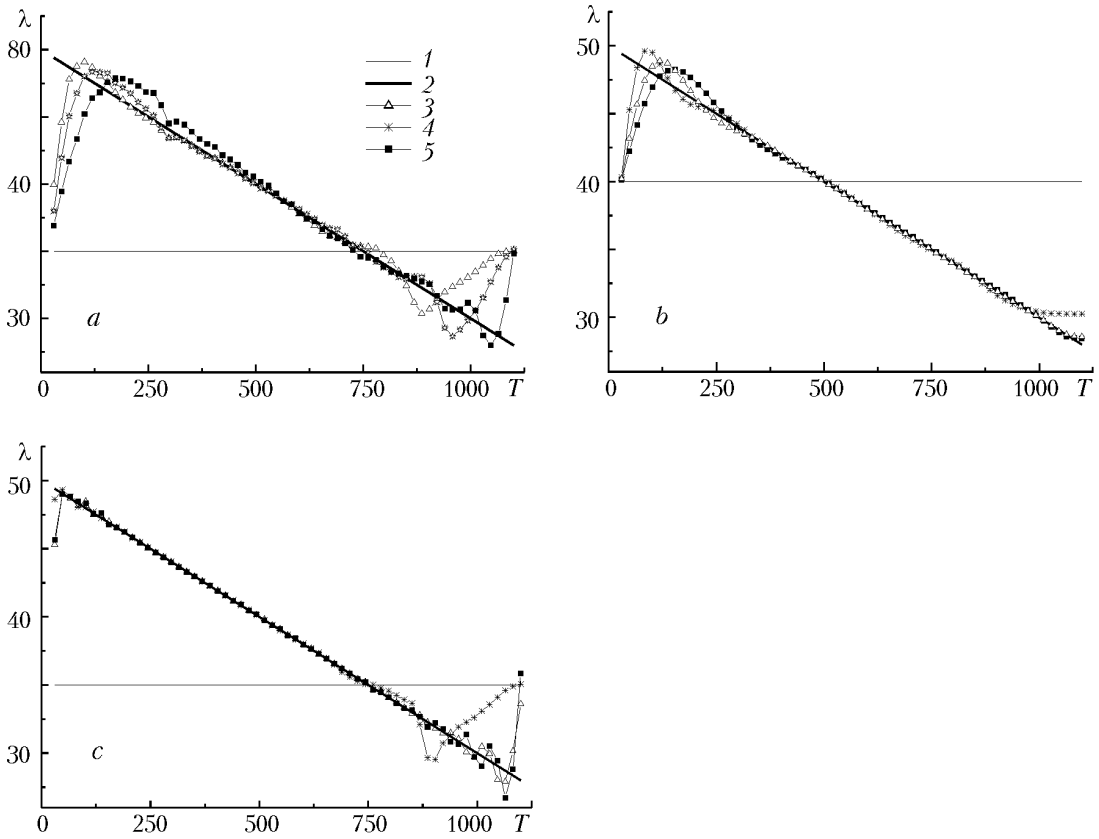

Fig. 3. Results of calculation of the thermal-conductivity coefficient according to algorithm I (a), according to algorithm II (b), and according to algorithm III (c): 1) λ_0; 2) λ_m; 3–5) λ_n [3) $x_*^1 = 0.025$; 4) $x_*^2 = 0.135$; 5) $x_*^3 = 0.25$]. λ, W/(m^3·°C); T, °C.

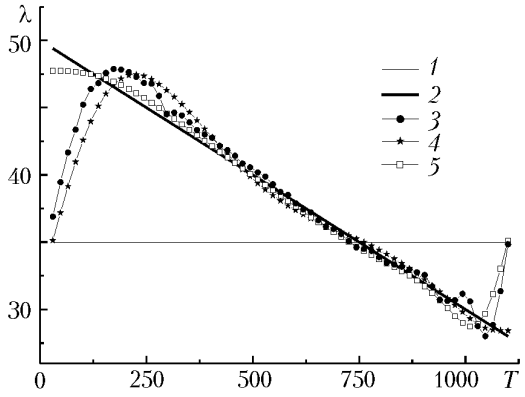

Fig. 4. Results of restoration of the thermal-conductivity coefficient for the point $x_* = 0.135$ according to algorithms I (1), II (2), and III (3) and their comparison to the zero approximation λ_0 (4) and the model function λ_m (5). λ, W/(m^3·°C); T, °C.

upon the attainment of which the algorithm halts.

The exactness of the solution on the right-hand or left-hand end of the temperature interval increases if the point of measurement of the temperature x_* is located closer to one end of the interval [0, b], and also depends on selection of the initial approximation. This is characteristic of the algorithms in question. However, the number of it-

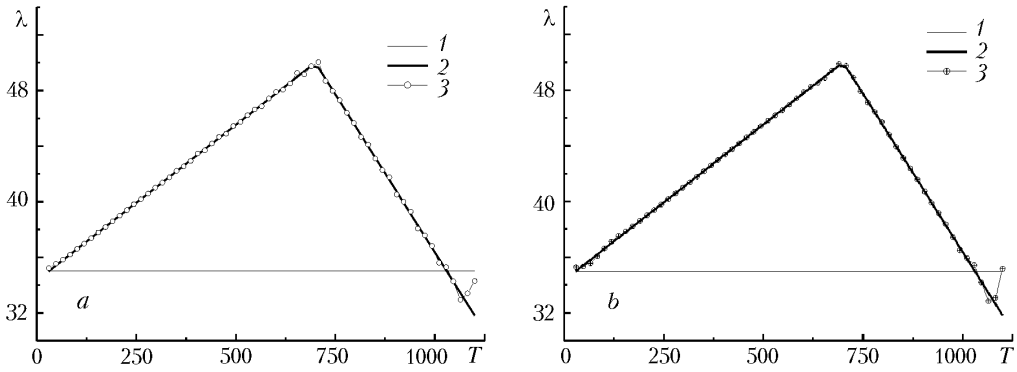

Fig. 5. Results of numerical restoration of $\lambda(T)$ with a discontinuous value $\frac{\partial \lambda}{\partial T}$ according to algorithm I (a) and according to algorithm III (b): 1) λ_0; 2) λ_m; 3) λ_{15} (a) and λ_{4015} (b). λ, W/(m^3.^{o}C); T, ^{o}C.

TABLE 1. Number of Iterations for Finding the Model Function (10)

λ_0	$x*$		
	0.025	0.135	0.2
45.0	315	440	359
49.0	110	225	128

erations necessary for attainment of the prescribed exactness, depending on the selection of the point x_*, is significantly different for different algorithms: in algorithm I, the number of iterations is small and virtually independent of the selection of the point x_*; in the case of algorithms II and III, the number of iterations necessary for attainment of the exactness indicated substantially depends not only on the selection of the point x_* but on the selected initial approximation λ_0 as well. The dependence of the number of iterations on the location of the point x_* and the selected initial approximation λ_0 in the case of the model function (10) for algorithm II is presented in Table 1.

The results of the numerical experiment with the use of accurate input data enable us to state that the method yields a nonuniform approximation for $\lambda(T)$, which, in principle, reflects the general properties of the gradient methods of solution of ill-posed problems [2–4]. This nonuniformity manifests itself as boundary effects: depending on the form of the algorithm (I, II, or III), the $\lambda_n(T^{(1)})$ and $\lambda_n(T^{(2)})$ values at the limiting points of the interval of variation of $\lambda(T)$ are close to the initial approximation. The nonuniformity of the approximation of $\lambda_n(T)$ to $\lambda(T)$ occurs on both ends of the interval of variation of λ in algorithm I, at the left end in algorithm II, and at the right end in algorithm III (see Figs. 3–5). An analysis of the character of nonuniformity of the approximation to the solution sought suggests the possibility of combining numerical results obtained through algorithms I, II, and III to find a more accurate approximation of $\lambda(T)$ at the ends the interval $[T^{(1)}, T^{(2)}]$ or refining the results in the case of the existence of breakpoints on the plot of the function $\lambda(T)$. For this purpose, we subdivide the domain of definition of the function $\lambda(T)$ into three or (in the case of the absence of breakpoints) two half-open intervals. Then the function $\lambda(T)$ may be represented in the form

$$\lambda(T) = \chi_1(T)\,\lambda^3(T) + \chi_2(T)\,\lambda^1(T) + \chi_3(T)\,\lambda^2(T),$$

where $\chi_i(T) = \begin{cases} 1 & \text{at } T \in [T_{(i)}, T_{(i+1)}], \\ 0 & \text{at } T \notin [T_{(i)}, T_{(i+1)}) \end{cases}$, $T_{(1)} = \min\limits_{(x,t)\in\partial\Omega} T(x,t)$, $T_{(4)} = \min\limits_{(x,t)\in\partial\Omega} T(x,t)$, $T_{(1)} < T_{(2)} < T_{(3)} < T_{(4)}$; $\lambda^i(T)$ is the solution of the inverse heat-conduction problem obtained using the ith variant of the algorithm.

The influence of the error of the input data on the solution of the inverse heat-conduction problem was investigated using quasiperiodic high-frequency disturbances of the function $y(t)$ input for the algorithms. The input data

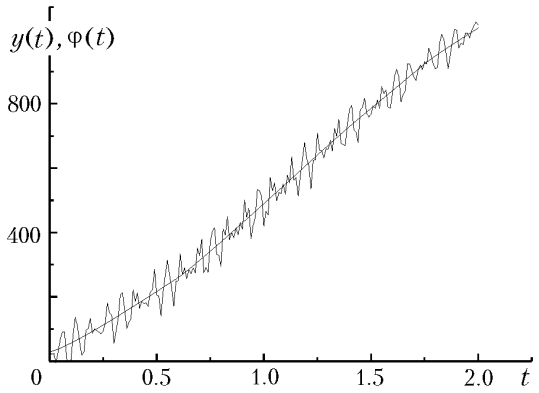

Fig. 6. Exact $y(t)$ and noise-affected $\varphi(t)$ values of the input data. $y(t)$ and $\varphi(t)$, ^{o}C; t, h.

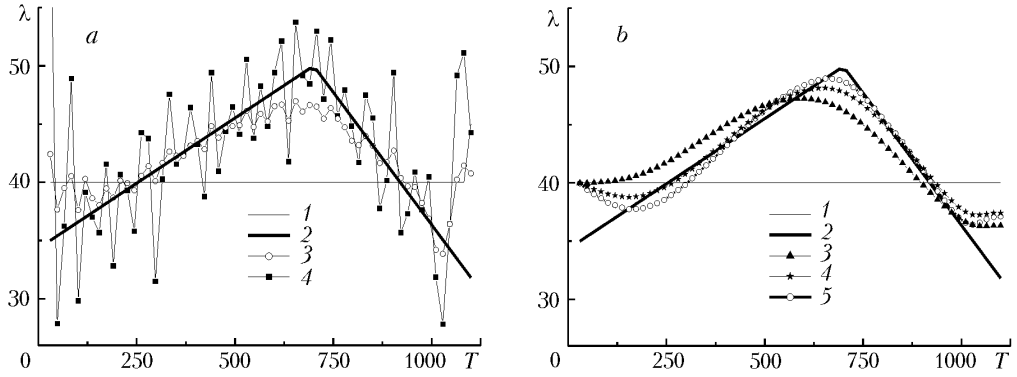

Fig. 7. Influence of the noise-affected input data on the results of calculation of the thermal-conductivity coefficient according to algorithm I (a) [1) λ_0; 2) λ_m; 3) λ_3; 4) λ_{15}] and algorithm II (b) [1) λ_0; 2) λ_m; 3) λ_{21}; 4) λ_{331}; 5) λ_{21}]. λ, W/(m^3·^{o}C); T, ^{o}C.

were used in the form $\varphi(t) = y(t) + \sum_{i=1}^{n} a_i \sin \omega t$, where $n = 5$, $\max_i a_i = 10.905$, and $\max_i \omega_i = 144{,}425.0$. The maximum value of the disturbance was 79^{o}C. Figure 6 presents the functions $y(t)$ and $\varphi(t)$ of the accurate and noise-affected input data for the case $\lambda_m(T)$ in the form (11). As a result of the calculations carried out, we have revealed the necessity of coordinating the value of the residual (12) with the level of noise to halt the operation of algorithm I (Fig. 7a). As far as algorithms II and III are concerned, we have established the stability of operation of these algorithms to the disturbances of input data virtually for any real value of the residual (12) (Fig. 7b).

Conclusions. The method (considered in this work) of determination of $\lambda(T)$ is highly efficient. Algorithms II and III, related to evaluation of $\lambda(T)$ in the Sobolev space $W_2^1[T^{(1)}, T^{(2)}]$ of absolutely continuous functions, deserve particular attention, since they demonstrate numerical stability in a wide range of disturbances of the input data of the problem. Also, it should be noted that the algorithms proposed enable us to restore the thermal-conductivity coefficients with a discontinuous temperature derivative, which is of great practical interest.

NOTATION

b, length of the segment, m; $c(T)$, heat-capacity coefficient, (W·h)/(m^3·^{o}C); N_x, number of nodes in the spatial variable; N_t, number of nodes in the temporal variable; t, running instant of time, h; t_f, final instant of time, h; T, temperature, ^{o}C; x, space coordinate, m; x_*, point of measurement of the temperature, m; $y(t)$, accurate input data, ^{o}C; w,

element of the Hilbert space; β_n, descent coefficient; $\delta(x - x_*)$, Dirac function; $\lambda(T)$, thermal-conductivity coefficient, W/(m·°C); λ_0, zero approximation; λ_n, nth approximation; λ_m, model function; ε_n, residual; $\varphi(t)$, noise-affected input data, °C; Ω, domain of definition; Λ, Hilbert space. Subscripts: f, final; m, model.

REFERENCES

1. V. T. Borukhov and V. I. Timoshpol'skii, Functional identification of the nonlinear thermal-conductivity coefficient by gradient methods. I. Conjugate operators, *Inzh.-Fiz. Zh.*, **78**, No. 4, 68–74 (2005).
2. O. M. Alifanov, *Identification of Heat-Transfer Processes of Flying Vehicles* (*Introduction to the Theory of Inverse Heat Transfer Problems*) [in Russian], Mashinostroenie, Moscow (1979).
3. O. M. Alifanov, *Inverse Problems of Heat Transfer* [in Russian], Mashinostroenie, Moscow (1988).
4. O. M. Alifanov, E. A. Artyukhin, and S. V. Rumyantsev, *Extremal Methods for Solving Ill-Posed Problems* [in Russian], Nauka, Moscow (1988).
5. A. A. Samarskii, *The Theory of Difference Schemes* [in Russian], Nauka, Moscow (1977).
6. B. E. Neimark, *Physical Principles of Steel and Alloys Used in Power Engineering: Handbook* [in Russian], Énergiya, Moscow–Leningrad (1967).
7. V. I. Timoshpol'skii, I. A. Trusova, and M. Ya. Pekarskii, *Annular Furnaces: Theory and Calculations* [in Russian], Vyshéishaya Shkola, Minsk (1993).